Amplitude sensing with a trapped-ion mechanical oscillator

K. A. Gilmore,[1,2,*] J. G. Bohnet,[1] B. C. Sawyer,[3] J. W. Britton,[4] and J. J. Bollinger[1]

[1] *National Institute of Standards and Technology, Boulder, Colorado 80305, USA*
[2] *JILA and Department of Physics, University of Colorado, Boulder, Colorado, 80309, USA*
[3] *Georgia Tech Research Institute, Atlanta, Georgia 30332, USA*
[4] *U.S. Army Research Laboratory, Adelphi, Maryland 20783, USA*

(Dated: January 18, 2017)

We present experimental and theoretical results demonstrating sensing with our trapped-ion mechanical oscillator of 50 pm displacement amplitudes, two orders of magnitude smaller than the ground state wavefunction size. Our system is a 2-D array of $^9Be^+$ ions in a Penning trap whose valence electron spins are coupled via a spin-dependent optical dipole force to the motional state of the ions. By reading out the dephasing of the spins, we are able to detect small displacements of the ion crystal. We document excellent theoretical agreement for the lineshapes, signal sizes, and sensitivity of our experiment. We perform these measurements off-resonantly and phase incoherently, but with near-term improvements expect to detect on-resonance sub-yN forces.

Measuring the amplitude of mechanical oscillators has engaged physicists for more than 50 years [1] and, as the limits of amplitude sensing have dramatically improved, produced exciting advances both in fundamental physics and in applied work. Examples include the detection of gravitational waves [2], the coherent quantum control of mesoscopic objects [3], improved force microscopy [4], and the transduction of quantum signals [5]. During the past decade, optical-mechanical systems have demonstrated increasingly sensitive techniques for reading out the amplitude of a mechanical oscillator, with a recent demonstration obtaining a precision more than two orders of magnitude below the size of the ground state wave function (i.e. the amplitude of the zero-point fluctuations) [6]. While optomechanical systems have assumed a wide range of physical systems, including toroidal resonators, nanobeams, membranes and others, the basic principle involves coupling the amplitude of a mechanical oscillator to the resonant frequency of an optical cavity mode [3].

Crystals of laser-cooled, trapped ions behave as atomic-scale mechanical oscillators [7–9] with tunable oscillator modes and high quality factors ($> 10^4$) . Furthermore, the techniques of laser cooling enable ground state cooling of these oscillators. Trapped-ion crystals therefore provide an ideal experimental platform for investigating the fundamental limits of amplitude sensing, but to date there have only been a handful of investigations [8–11]. These investigations demonstrate amplitude detection comparable to or larger than the zero-point fluctuations of the trapped-ion oscillator.

In this Letter we experimentally and theoretically analyze a technique with which the center-of-mass (COM) motion of a 2-dimensional, trapped-ion crystal of ∼100 ions can be detected with a sensitivity several orders of magnitude below the zero-point fluctuations. Instead of coupling the motion to an optical mode of a cavity, we employ a time-varying spin-dependent force that couples the amplitude of the COM motion with internal spin degrees of freedom of the ions [12, 13]. When the frequency μ of the spin-dependent force matches the frequency ω of an imposed COM oscillation, $Z_c \cos(\omega t)$, spin precession proportional to Z_c occurs, which we read out with a precision imposed by spin projection noise [14]. Analogous to the canonical optomechanical coupling, here the amplitude of the trapped-ion oscillator produces a shift in the frequency of the spin (or qubit) degree of freedom of the trapped ions.

To demonstrate the sensitivity of this technique in the absence of noise and excitations of the COM mode, we perform measurements where ω is far from resonance with the mechanical COM resonance frequency ω_z of the ion array. We demonstrate a sensitivity of $(100\text{ pm})^2/\sqrt{Hz}$ and the detection of amplitudes Z_c as small as 50 pm, almost two orders of magnitude below the ∼2 nm ground state wave function size. For our set-up a 50 pm amplitude at a frequency ω far from resonance corresponds to an electric field detection of 0.46 mV/m or 73 yN/ion. These force and electric field sensitivities can be improved by the Q of the COM mode by probing near resonance with ω_z. Further improvements can be obtained using techniques such as spin-squeezing [15] to reduce projection noise of the readout.

Our experimental apparatus, described in Fig. 1 and [12, 15], consists of $N \sim 100$ $^9Be^+$ ions laser-cooled to the Doppler limit of 0.5 mK and confined to a single-plane Coulomb crystal in a Penning trap. The spin-1/2 or qubit degree of freedom is the $^2S_{1/2}$ ground-state valence electron spin $|\uparrow\rangle$ ($|\downarrow\rangle$) $\equiv |m_s = +1/2\rangle$ ($|m_s = -1/2\rangle$). In the magnetic field of the Penning trap, the ground state is split by 124 GHz. A resonant microwave source is used to perform global rotations of the spin ensemble. A pair of laser beams, detuned from any optical transitions by ∼20 GHz, interfere to form a 1-dimensional optical lattice, resulting in a spin-dependent optical dipole force (ODF) that couples the spins to the ions's axial motion. The cooling and repump transitions allow for efficient preparation of all N trapped ions to the state $|\uparrow\rangle_N \equiv$

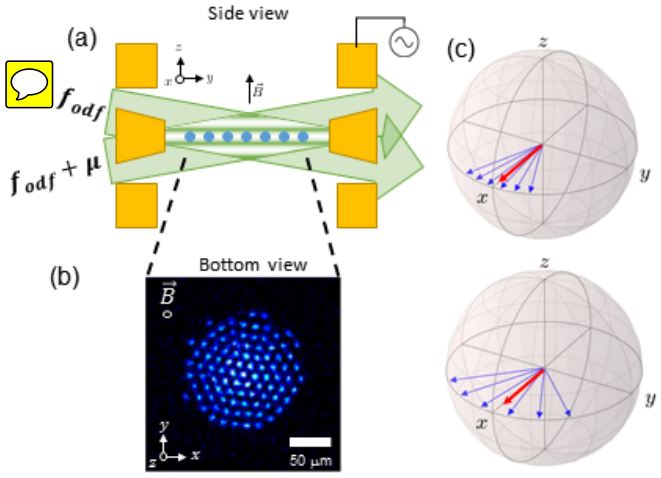

FIG. 1. (a) Cross-section of the NIST Penning trap, characterized by an axial magnetic field $B = 4.45$ T and an axial trap frequency $\omega_z = 2\pi \times 1.57$ MHz. The blue dots represent the ions. Cylindrical electrodes (yellow) generate a harmonic confining potential along their axis. Radial confinement is provided by the Lorentz force from $\vec{E} \times \vec{B}$-induced rotation in the axial magnetic field. ~~Time varying potentials applied to eight azimuthally segmented electrodes generate a rotating wall potential that controls the crystal rotation frequency.~~ Doppler cooling beams are directed along y and z. The beams generating the spin-dependent optical dipole force cross the ion plane at $\pm 10°$, forming a 1-dimensional optical lattice (green lines) with a 0.9 μm wavelength. ~~Global, state-dependent fluorescence is collected on the side-view objective.~~ (b) Bottom-view image of ion crystal. (c) Dephasing of the spins after rotation to the equator of the Bloch sphere. Each blue vector represents an experimental trial and the green vector the average of the $\hat{x}$ component. Due to the incoherent nature of our experiment, the measurement is sensitive to this averaged Bloch vector. The maximum angle of precession, θ_{max}, is determined by the amplitude of the displacement of the oscillator. This is represented by the spread in blue vectors in the top (small displacement) and bottom (large displacement) Bloch spheres.

$|\uparrow\uparrow \cdots \uparrow\rangle$. At the end of the experiments described here we measure the average probability $P_\uparrow$ for an ion spin to be in $|\uparrow\rangle$ from a global measurement of state-dependent resonance fluorescence on the Doppler cooling transition. ~~This is equivalent to measuring the z-component of the composite Bloch vector of the spins.~~

The ODF couples the spin and motional degrees of freedom through the interaction [15]

$$H_{ODF} = U \sum_i \sin(\delta k \cdot \hat{z}_i - \mu t + \phi)\hat{\sigma}_i^z, \qquad (1)$$

where δk is the wave vector describing the 1D optical lattice, μ (ϕ) is the frequency (phase) difference between the ODF beams, and $\hat{z}_i$ and $\hat{\sigma}_i^z$ are the position operator and Pauli spin matrix for ion i. We work in a regime where Lamb-Dicke confinement is approximately satisfied, $\delta k \left\langle \hat{z}_i^2 \right\rangle^{1/2} \lesssim 0.5$. In this case, and assuming $U/\mu \ll 1$, Eq. 1 can be approximated as

$$H_{ODF} \approx U \sum_i \sin(\delta k \cdot \hat{z}_i) \cos(\mu t - \phi)\hat{\sigma}_i^z. \qquad (2)$$

With ~~an rf tickle~~ on one of the trap electrodes at a frequency ω far from any of the axial drumhead modes, we impose a weak, classically driven COM motion of constant amplitude and phase, $\hat{z}_i \to \hat{z}_i + Z_c \cos(\omega t + \delta)$. With $\delta k Z_c \ll 1$ and assuming $\mu \sim \omega$, Eq. 2 can be simplified to describe the shift in the qubit transition frequency due to the coherent amplitude Z_c,

$$H_{ODF} = DWF \cdot U \cdot \delta k \cdot Z_c \cos((\omega - \mu)t + \delta + \phi) \sum_i \frac{\hat{\sigma}_i^z}{2}. \quad (3)$$

Here $DWF \equiv \exp(-\delta k^2 \left\langle \hat{z}_i^2 \right\rangle /2) \approx 0.86$ is the Debye-Waller factor, a reduction in interaction strength due to the departure from the Lamb-Dicke confinement regime [16].

For $\mu = \omega$ there is a static shift $\Delta(Z_c)$ in the frequency of the qubit transition,

$$\Delta(Z_c) = DWF \cdot (U/\hbar) \cdot \delta k \cdot Z_c \cos(\delta + \phi). \qquad (4)$$

For the moment, we assume $\delta + \phi = 0$. Then $\Delta(Z_c)$, ~~the zero-point fluctuations of the COM mode for $N = 100$~~ evaluated at $Z_c = \frac{1}{\sqrt{N}} \sqrt{\frac{\hbar}{2m\omega_z}} \approx 1.9$ nm, is the equivalent vacuum optomechanical coupling strength g_0 [3] for our set-up. With $\delta k = 2\pi/900$ nm (see Fig. 1) and a modest 1D lattice potential $U/\hbar = 2\pi \times (10\,kHz)$, typical of that employed here, $\Delta(1.9\,nm) \approx 710\ s^{-1}$. We measure $\Delta(Z_c)$ from the resulting spin precession in a Ramsey-style experiment like that discussed in Fig. 2. If τ is the total ODF interaction time of the sequence, the resulting spin precession on resonance ($\mu = \omega$) is simply $\theta = \theta_{max} \cos(\delta + \phi)$ where $\theta_{max} \equiv DWF \cdot (U/\hbar) \cdot \delta k\ Z_c \cdot \tau$.

Due to phase instabilities in our current implementation of the ODF interaction, we measure the induced spin precession phase incoherently. If the phase of the applied force was unknown or time-dependent, this phase-incoherent sensing would be necessary - and so, our experiment represents a 'worst-case' sensing experiment. In the phase-incoherent picture, the relative phase between the drive (δ) and the ODF beat note (ϕ) is sampled randomly with each repetition of the experiment. Different experimental trials therefore result in a different precession $\theta = \theta_{max} \cos(\phi + \delta)$. We measure the decrease (or decoherence) in the average length of the Bloch vector resulting from this random precession. In a Ramsey sequence where a Bloch vector undergoing no precession is rotated to the dark state $|\downarrow\rangle_N$ (see Fig. 2), the average probability for measuring spin-up is $\langle P_\uparrow \rangle = \frac{1}{2}[1 - e^{-\Gamma\tau} \langle \cos(\theta) \rangle]$. Here $\Gamma = \frac{1}{2}(\Gamma_{el} + \Gamma_{ram})$ is the decay rate from spontaneous emission from the

off-resonant ODF laser beams, where Γ_{el} (Γ_{ram}) is the elastic (Raman) scattering decoherence rate [17]. The average $\langle\cos(\theta)\rangle$ is over the random phase $\phi+\delta$ with the result $\langle\cos(\theta)\rangle = J_0(\theta_{max})$, where J_0 is the zeroth order Bessel function of the first kind. Thus,

$$\langle P_\uparrow\rangle = \frac{1}{2}\left[1 - e^{-\Gamma\tau}J_0(\theta_{max})\right]. \quad (5)$$

We note that the incoherent sensing described by Eq. 5 is second-order sensitive to θ_{max} (or Z_c).

To create the steady-state COM axial oscillation $Z_c\cos(\omega t+\delta)$, we applied a continuous AC voltage (i.e. an rf tickle) to an endcap of the Penning trap at a frequency near $\omega/(2\pi) =$ 400 kHz. This frequency was chosen because it was far from any mode frequencies of the array, and there were no observed sources of noise. Specifically application of the ODF interaction with $\mu/(2\pi) \approx 400$ kHz and no rf tickle resulted in a background given by $\langle P_\uparrow\rangle_{bck} = \frac{1}{2}\left[1-e^{-\Gamma\tau}\right]$. Characterization of the detection sensitivity requires calibration of the applied AC voltage in terms of ion displacement. We calibrated the displacement of the ions due to a static voltage applied to the endcap by measuring the resulting movement of the ion crystal in the side-view imaging system. From this calibration, we determine that a 1 V offset results in a 0.97 $\pm$ 0.009 μm displacement of the ions. We estimate that the corrections for using this DC calibration with an $\omega/(2\pi) \approx 400$ kHz drive is less than 10%.

Our experimental sequence makes use of the quantum lock-in technique wherein the phase accumulated due to spin-precession in each arm of the sequence is added coherently [18]. To decouple from magnetic field fluctuations over the course of the experiment, a spin echo style sequence is used. Figure 2 shows a CPMG sequence - a multipulse extension of the Hahn spin echo - with two π pulses and phase jumps appropriate for adding the accumulated phases. The general experimental sequence is as follows. A calibrated drive at ∼400 kHz is applied to the endcap of the trap and left on throughout the experiment. The ions are prepared in $|\uparrow\rangle_N$ with cooling and repump lasers. A microwave $\pi/2$ pulse rotates the spins to the $\hat{x}$ axis, to the superposition $\left[|\uparrow\rangle_N + |\downarrow\rangle_N\right]/\sqrt{2}$. The ODF beams are pulsed on for a duration T followed by a microwave π pulse about $\hat{x}$ and another ODF pulse of duration T. This ODF-π-ODF sequence is repeated n times. After a second $\pi/2$ pulse about $\hat{y}$, the final state readout measures the population of the spins in $|\uparrow\rangle$ through global fluorescence. Using $n = 8$ ODF-π-ODF pulses allows us to push the sequence time out to 20 ms and maintain a background fully characterized by decoherence due to spontaneous emission.

To model the lineshape of the signal, it is necessary to account for the accumulated phase due to the spin-dependent ODF potential without making the simplification that $\omega = \mu$. This results in a characteristic response function for each sequence. The response function relevant for the $n = 8$ CPMG sequence is derived in the supplementary materials. Figure 2 (c) shows the evolution of the signal relative to the background as the power of the ODF beams is increased. Figure 2 (d) shows the emergence of the signal out of the background as the drive amplitude is increased. In both cases the theory has no free parameters. The background is accounted for by independent measurements of spontaneous emission. The spontaneous emission decay rates are calculated from the measured AC Stark shifts induced by each ODF laser beam, a proxy for the laser intensity at the ions.

With the drive frequency chosen to satisfy $\omega/2\pi = (2n+1)/(2(T+t_\pi))$, scanning the power of the ODF laser varies the strength of the measurement. By comparing $\langle P_\uparrow\rangle$ and $\langle P_\uparrow\rangle_{bck}$, as in Fig. 2 (c), the signal and the signal-to-noise can be extracted. From this, the sensitivity of the sequence is found. To calculate the signal-to-noise ratio, a value for θ^2_{max} needs to be extracted. Defining $F\left(\theta^2_{max}\right) \equiv \frac{1}{2}\left(1 - J_0\left(\theta_{max}\right)\right)$, solving for θ^2_{max} requires a measurement of the difference $\langle P_\uparrow\rangle - \langle P_\uparrow\rangle_{bck}$ through

$$F\left(\theta^2_{max}\right) = e^{\Gamma\tau}\left(\langle P_\uparrow\rangle - \langle P_\uparrow\rangle_{bck}\right). \quad (6)$$

The signal-to-noise for a single experiment is given by $\theta^2_{max}/\delta\theta^2_{max}$. The signal-to-noise (see Supplemental Materials for details) is maximized for small values of θ^2_{max}, such that $F\left(\theta^2_{max}\right) \approx \theta^2_{max}/8$ is a valid approximation. As a result, we estimate the signal-to-noise ratio of a single measurement as

$$\frac{\theta^2_{max}}{\delta\theta^2_{max}} \approx \frac{\langle P_\uparrow\rangle - \langle P_\uparrow\rangle_{bck}}{\delta\left(\langle P_\uparrow\rangle - \langle P_\uparrow\rangle_{bck}\right)}. \quad (7)$$

For large amplitude displacements, the shot-to-shot fluctuations of the relative phase of the 1D optical lattice and driven COM motion is the dominate noise and the signal-to-noise is limited to ~ 1. As the drive amplitude is decreased, the relative contribution of this random phase to the noise decreases as well, and the projection noise becomes dominant. In this regime, the signal-to-noise ratio begins to decrease, representing the limit of sensitivity for this experiment.

To explore the ultimate limits of sensitivity of our setup, we repeat the aforementioned experimental sequence first without the applied drive on - to get the background - and then with the drive. For a particular applied drive with known calibrated ion displacement, the experimental sequence is repeated 3000 times. Using Eq. 7, the experimental signal-to-noise is calculated by taking the difference $\langle P_\uparrow\rangle - \langle P_\uparrow\rangle_{bck}$ of sequential pairs of experiments and dividing by the standard deviation of these differences. We plot the experimental signal-to-noise as a function of ion displacement in Fig. 3. Our theoretical predictions (detailed in the Supplemental Materials) assume the only sources of noise are projection

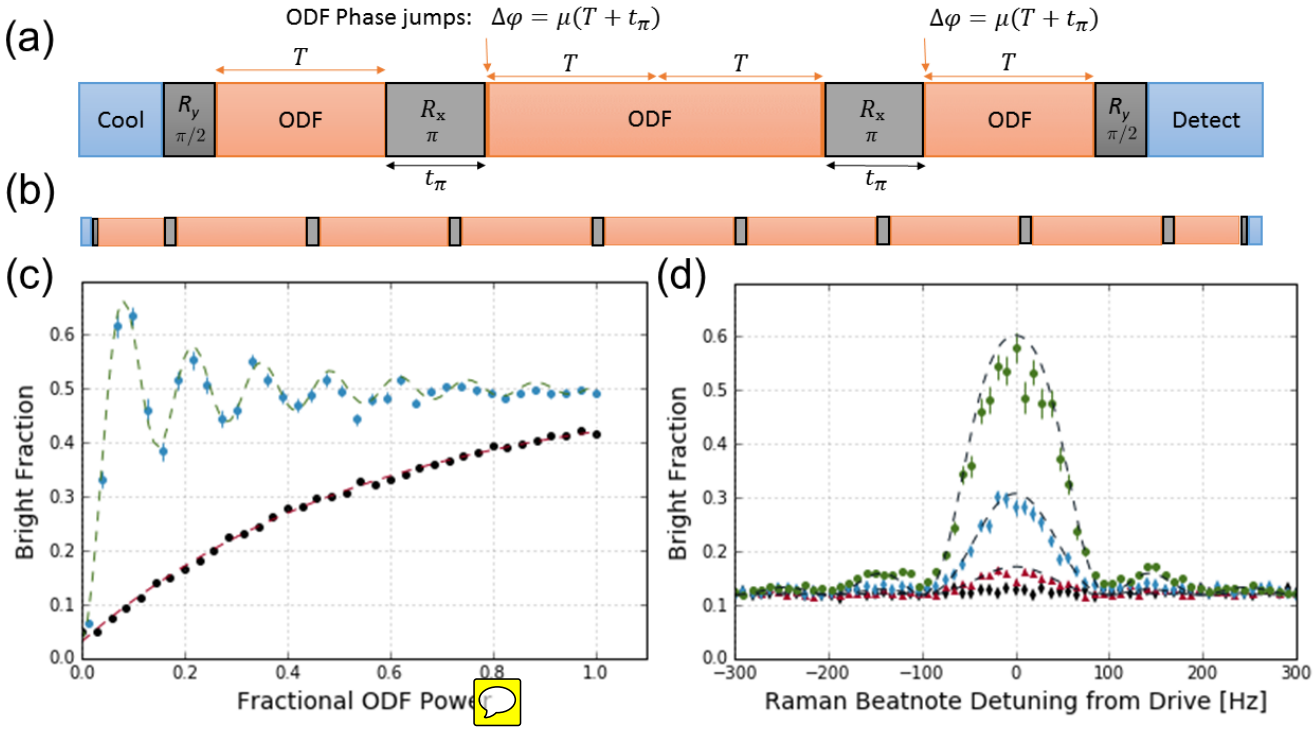

FIG. 2. (a) CPMG sequence with two π pulses. Orange blocks represent ODF pulses, grey microwave rotations, and blue cooling and ~~detecting~~. ~~In this experiment, the classical drive is left on throughout~~. After each π pulse, the ODF phase is jumped by $\Delta\varphi = \mu(T + t_\pi)$, which cancels a term in the Hamiltonian relevant at low frequencies μ (when the approximation $U/\mu \ll 1$ does not hold) so that Eq. 2 remains valid. For $\mu/2\pi = (2n+1)/(2(T+t_\pi))$, $\Delta\varphi = \pi$ and therefore spin precession is coherently accumulated for $\omega/2\pi = (2n+1)/(2(T+t_\pi))$. (b) CPMG sequence with 8 π pulses. Cooling and detection remain the same, and the phase is jumped by the same amount after each π pulse. Chaining the ODF pulses in this fashion allows us to go to much longer total interaction times (20 ms, for $T = 1.25$ ms) and detect smaller displacements for a given interaction U. (c) As a function of measurement strength (ODF power), the background (black points) with no applied drive and signal (blue points) for a 2.5 nm displacement is shown. The red curve is a fit to the background. The green curve is the theoretical prediction given the background with no free parameters. The oscillations are due to the Bessel function behavior of the signal. (d) Lineshape of the classical drive for drive amplitudes of 500 pm (red), 1 nm (blue) and 2 nm (green). Black points are background, with drive turned off. Dashed lines are theory curves with no free parameters. All error bars represent standard error.

noise in the spin state measurement and fluctuations in $P_\uparrow$ caused by the incoherence between the phase of the applied drive and the ODF beatnote.

In summary, we have presented a novel technique for amplitude and force sensing. By isolating and controlling a two-level system comprised of the effective spin-1/2 in each ion in our Penning trap and applying a global spin-dependent force, the spin and motional degrees of freedom of the ions are coupled and the motional state of the ions may be directly read out from the spin state. We have documented, with excellent theoretical agreement, the response of our trapped-ion mechanical oscillator to an applied off-resonant drive and demonstrated a projection noise limited sensitivity of $(100\ \text{pm})^2/\sqrt{\text{Hz}}$ and the detection of amplitudes Z_c as small as 50 pm, almost two orders of magnitude below the ~2 nm ground state wave function size. Though our experiments are performed phase-incoherently and off-resonantly, with near-term improvements we expect to operate phase-coherently and on resonance with the center of mass mode frequency of the ion crystal. We expect such improvements to improve the limiting sensitivity to $\sim (20\ \text{pm})/\sqrt{\text{Hz}}$. This would enable us to make use of recently demonstrated spin-squeezing in our ensemble of 100s of ions [15] to perform further quantum enhanced sensing [13] and improve $\theta_{max}/\delta\theta_{max}$ by a factor of two. In addition, further improved sensitivity is possible with reduction of spontaneous emission, Γ, relative to the interaction strength, U. When μ is applied on resonance with ω_z, the force and electric field sensitivities can be improved by the Q of the COM mode, which we estimate as $Q \sim 10^4$ for our set-up. The detection of a 20 pm amplitude resulting from a 5 ms coherent drive on the 1.57 MHz COM mode is sensitive to a force/ion of 10^{-3} yN corresponding to an electric field of 7 nV/m. Thus in the near future, we can demonstrate with phase-

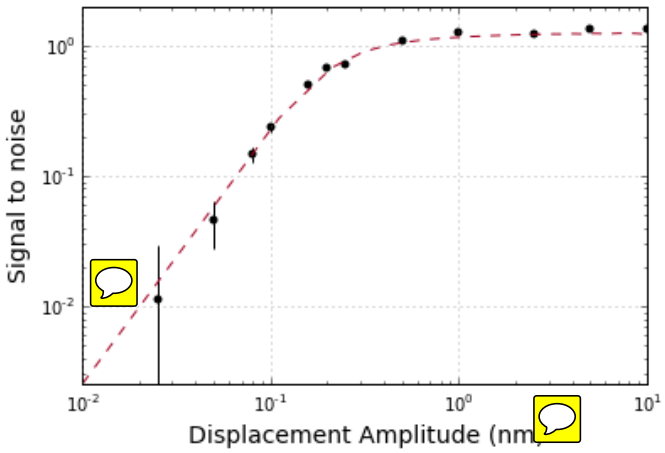

FIG. 3. Limit of amplitude sensing for N = 85 ions. Our measured sensitivity of $(100\,\mathrm{pm})^2/\sqrt{\mathrm{Hz}}$ is limited by projection noise in the spin state detection. As the amplitude of the applied drive is decreased, the projection noise of the spin ensemble dominates and the signal-to-noise ratio decreases. At larger amplitudes, the shot-to-shot fluctuations of the precession angle θ^2 limit the signal-to-noise ratio to ~ 1. Error bars represent the standard error.

coherent detection amplitude sensing below the standard quantum limit and the sensing of forces orders of magnitude smaller than a yN.

* kevin.gilmore@colorado.edu

[1] J. Weber, Physical Review Letters **17**, 1228 (1966).

[2] B. P. Abbott and et al, Phys. Rev. Lett. **116**, 61102 (2016), arXiv:1602.03837.

[3] M. Aspelmeyer, T. J. Kippenberg, and F. Marquardt, Reviews of Modern Physics **86**, 1391 (2014), arXiv:0712.1618.

[4] H.-J. Butt, B. Cappella, and M. Kappl, Surface Science Reports **59**, 1 (2005).

[5] T. A. Palomaki, J. W. Harlow, J. D. Teufel, R. W. Simmonds, and K. W. Lehnert, Nature **495**, 210 (2013), arXiv:arXiv:1206.5562v1.

[6] D. J. Wilson, V. Sudhir, N. Piro, R. Schilling, a. Ghadimi, and T. J. Kippenberg, Nature **524**, 325 (2014), arXiv:1410.6191.

[7] J. D. Jost, J. P. Home, J. M. Amini, D. Hanneke, R. Ozeri, C. Langer, J. J. Bollinger, D. Leibfried, and D. J. Wineland, Nature **459**, 683 (2009), arXiv:0901.4779.

[8] M. J. Biercuk, H. Uys, J. W. Britton, A. P. VanDevender, and J. J. Bollinger, Nature nanotechnology **5**, 646 (2010), arXiv:1004.0780.

[9] B. C. Sawyer, J. W. Britton, A. C. Keith, C.-C. J. Wang, J. K. Freericks, H. Uys, M. J. Biercuk, and J. J. Bollinger, Physical Review Letters **108**, 213003 (2012), arXiv:arXiv:1201.4415v1.

[10] R. Shaniv and R. Ozeri, ArXiv e-prints arXiv:1602.08645 , 1 (2016), arXiv:arXiv:1602.08645v1.

[11] S. Knünz, M. Herrmann, V. Batteiger, G. Saathoff, T. W. Hänsch, K. Vahala, and T. Udem, Physical Review Letters **105**, 1 (2010).

[12] B. C. Sawyer, J. W. Britton, and J. J. Bollinger, Physical Review A - Atomic, Molecular, and Optical Physics **89** (2014), 10.1103/PhysRevA.89.033408, arXiv:1401.0672.

[13] P. A. Ivanov, Physical Review A **94**, 022330 (2016), arXiv:1606.07299.

[14] W. M. Itano, J. C. Bergquist, J. J. Bollinger, J. M. Gilligan, D. J. Heinzen, F. L. Moore, M. G. Raizen, and D. J. Wineland, Physical Review A **47**, 3554 (1993).

[15] J. G. Bohnet, B. C. Sawyer, J. W. Britton, M. L. Wall, A. M. Rey, M. Foss-feig, and J. J. Bollinger, arXiv e-prints , 1 (2015), arXiv:1512.03756.

[16] D. J. Wineland, C. Monroe, W. M. Itano, D. Leibfried, B. E. King, and D. M. Meekhof, Journal of Research of the National Institute of Standards and Technology [J. Res. Natl. Inst. Stand. Technol **103**, 1689 (1998), arXiv:9710025 [quant-ph].

[17] H. Uys, M. J. Biercuk, a. P. Vandevender, C. Ospelkaus, D. Meiser, R. Ozeri, and J. J. Bollinger, Physical Review Letters **105**, 1 (2010), arXiv:1007.2661.

[18] S. Kotler, N. Akerman, Y. Glickman, A. Keselman, and R. Ozeri, Nature **473**, 61 (2011), arXiv:1101.4885.